This manuscript is a **preprint** and has been submitted to the **Journal of Hydrology**. Please note that this manuscript is undergoing peer-review, and has not been accepted for publication. Subsequent versions of this manuscript may have slightly different content. If accepted, the final version of this manuscript will be available via the 'Peer-reviewed Publication DOI' link on the right-hand side of this webpage. Please feel free to contact the corresponding author. We appreciate your feedback.

# Evaluating Controller Performance and Placement on System-level Urban Flooding Reduction and Water Quality Improvement

Jiada Li[a,*], Carlos Oroza[a], BrandonWong[b], Steven Burian[a]

[a]Department of Civil and Environmental Engineering, University of Utah, 201 Presidents Circle, Salt Lake City, UT, USA

[b]Department of Civil and Environmental Engineering, University of Michigan, Ann Arbor, MI, USA

[a,*] Corresponding author, email: jiada.li@utah.edu

## Highlights

1. A modified water quantity and quality co-simulation tool was tested by using EPA SWMM and Python;
2. A methodology for assessing the performance of rule-based system-level real-time control was developed to obtain global benefits;
3. System-level control outperforms individual control in solving system-level flooding and pollutant over-loading issues, but it needs more operation energy and may result in system instability;
4. An index considering both water quantity and quality factors were developed to design the controller placement strategy under rainfall variability.

**Abstract** Increases in urbanization and climate change are forcing urban drainage engineers to more effectively leverage stormwater storage facilities to minimize flooding and water quality impacts. This process becomes increasingly challenging due to the operations of storage coordination across the system-level watershed. This study presents a system-level real-time control simulation for assessing watershed-scale performance. The objective of this work is to make a trade-off between the flooding mitigation at flooded nodes and water quality stress reduction at storage ponds. An open-source tool called PySWMM was used to conduct control rule simulation and water quantity and quality modeling. For testing this tool, four rule-based control scenarios were performed: baseline control, the downstream individual control, system-level control with 11 same controllers, and system-level control with 11 different controllers. Meanwhile, three indicators, including peak depth shaving efficiency, pollutant removal efficiency, and flooded-hour reduction, were used to evaluate the controller performance in system-level operation coordination. A real-world and watershed-scale urban drainage system, called Network A, was selected as the case study. Our results indicate that the most downstream controller performs best in alleviating downstream flooding while the system-level controller has better performance in obtaining global benefits with a higher Peak Depth Shaving Efficiency (up to 7.30% ), Pollutant Removal Efficiency (up to 66.59%), and Flooded-hour Reduction (up to 71.01%). A quantitative controller placement analysis based on Controller Placement Index (CPI) was then conducted to determine which controllers have positive or negative effects on system-level outcomes. The CPI values suggest that upstream ponds with lower storage capacity should be regulated, while those downstream ponds with larger storage volumes ought to be uncontrolled, to maximize the global benefits. This paper provides a basis for improving the design of a system-level and watershed-scale controlled urban drainage systems.

*Keywords:* **Real-time control, Urban drainage systems, Flooding, Total suspended solids, PySWMM**

# 1.Introduction

Recently, climate change and anthropogenic activities are drastically challenging stormwater management practices by increasing the magnitude, frequency, and duration of extreme rainfall events (U.S. EPA, 2006). Such climate-related phenomena eventually trigger stormwater problems, for example, flashier hydrographs and pollutographs in the urbanized watershed (Waters et al., 2003). Urban stormwater has serious effects on UDSs (Urban Drainage Systems) such as flooding, water quality deterioration, infrastructure erosion, and ecosystem impairment (Schmitt et al., 2004). These impacts on stormwater runoff and water quality subsequently lead to more social, environmental and economic costs. For instance, 160 million U.S. dollars were utilized to plan for the potential stormwater projects in the coming years, enabling the utility to solve stormwater issues in southeast urbanized areas of Michigan, and annual stormwater fund revenues will increase by about 28% in the coming years (Santon, 2018). Therefore, it is of great importance to improve the existing UDSs to mitigate unexpected eco-hydraulic stress on water quantity and quality.

However, most existing UDSs, with limited conveyance capacity, are not adaptively designed to cope with such rapid water quantity and quality changes (Berggren et al., 2012). Traditionally, engineers tackle these issues by enlarging existing stormwater facilities or re-sizing physical structures in the stormwater infrastructure systems. Nevertheless, upgrades on grey infrastructures are costly for in-site construction (Casal-Campos et al., 2015). The disadvantages of stormwater structure rehabilitation are the adverse impacts on the receiving environment such as loss of open space and loss of permeable land (Li et al., 2019b). In order to diminish these effects, stormwater stakeholders are constantly looking for more dynamic stormwater solutions. One such alternative is non-structural RTC (Real-Time Control), which has been extensively explored for lessening water quality stress and mitigating flooding severity (Bilodeau et al., 2018; Giordano et al., 2014; Mollerup et al., 2017; Parolari et al., 2018).

Prior studies have considered RTC as an adaptive, efficient, and low-cost practice for optimizing the operational efficiency in water distribution system (Abou Rjeily et al., 2018; Creaco et al., 2019), adapting drainage system to changing conditions (Campisano et al., 2013; Löwe et al., 2016; Lund et al., 2019), and improving water quality in ecosystems (Zhang et al., 2018). With an interest in non-traditional stormwater management approaches, RTC has been applied widely for different purposes such as combined sewer overflow reduction, flooding mitigation, greenhouse gas emissions control, energy-saving, and TSS (Total suspended solids) removal (Chiang and Willems, 2015; Kroll et al., 2018; Muschalla et al., 2014; Ruggaber et al., 2007). Recent studies formulated the control rules to improve TSS removal efficiency from 41% to 89% (Sharior et al., 2019) and to reduce combined sewer overflow volume by up to 50% (Vezzaro and Grum, 2014). However, most of the techniques are based on individual control but not consider system-wide operations (Mullapudi et al., 2017). Individual control at the site-scale catchment is useful for flooding stress reduction and water quality improvement (Heusch and Ostrowski, 2015; van Overloop et al., 2005). Nevertheless, the outcomes might be questionable when the study scale is expanded from local to the system-level watershed.

Few studies focus on assessing controller performance considering water quantity and quality perspectives simultaneously (Kerkez et al., 2016; Vitasovic, 2006). Previous research focused on evaluating the system-level control strategy based on the simplified linear system. However, this simplification tends to ignore the physical hydraulic-hydrological dynamics of the stormwater system, which contains higher uncertainty in using models to represent real systems (Hashemy Shahdany et al., 2019; Wong and Kerkez, 2018). The latest studies find that developing an external programming wrapper connected with the SWMM (Storm Water Management Model) is beneficial for mimicking real UDSs and site-oriented control logics (Riaño-Briceño et al., 2016; Sadler et al., 2019b). It is necessary to develop a simulation approach that co-simulates rainfall-runoff dynamics and control logics. In addition, such multi-purposed global benefits might decline due to improper sites selected for the controller. Previous work has analyzed the method to identify the best candidate sites for the controller by ranking the system-wide performance improvement and increasing the number of controlled storage units to gain the maximum global benefits (Bartos and Kerkez, 2019; Wong and Kerkez, 2018). However, these studies identify the controller sites without considering the water quality aspects. Therefore, a better assessment of the controller performance and placement for mitigating flooding, and TSS loading is essential for system-level stormwater management. So far, limited attention has been paid to promote system-level RTC, enhancing global benefits in UDSs (Emerson et al., 2005; Meneses et al., 2018).

The objective of this study is to assess system-level controller performance in achieving simultaneous water quality stress reduction and flooding mitigation. This work also aims to locate the placement for those controllers with positive performance in reducing flooding and TSS loading. A real-world watershed-scale urban drainage system located in the Southeastern Michigan, U.S., was selected as the study case. The contributions of this study can be summarized as follows:

1) A co-simulation approach to simultaneously execute the rule-based control logic and water quality simulation through the modified PySWMM tool (McDonnell et al., 2017; Sharior et al., 2019).

2) An index-oriented assessment of real-time control strategies' performance towards the trade-off between reducing the flooding stress and improving the water quality.
3) A water quality-based method to identify where storage units should be controlled to obtain the best global control benefits, focusing specifically on shaving hydraulic peak depth, flooded hours, and alleviating total suspended solids loads.

The first contribution was achieved by simulating the system-level control strategy, used to explore the potential of concurrently reducing water quantity and quality over-loads. Implementing three indicators, Peak Depth Shaving Efficiency (PDSE), Pollutant Removal Efficiency (PRE), and Flooded-hour Reduction (FR), assesses the controller performance for the second accomplishment. The third contribution was made by using the Controller Placement Index (CPI) to assess controller location under different artificial rainfall patterns.

# 2. Study Area and Datasets

## 2.1 Study Case

In this study, a real-world, highly urbanized stormwater urban drainage system, located in southeastern Michigan state, U.S., was chosen as the study case. This creekshed consists of 11 interconnected stormwater basins that handle the runoff from each sub-catchment each. Fig.1 presents the SWMM model called (Network A) for representing the urban drainage system. This model includes 19 sub-catchments, 10 junctions, 1 outfall nearby the Huron river, 11 conduits, 11 orifices, and 11 storage units. Shown in Fig.1, two storage units, including SU2 and SU8, are detention ponds while the others are retention ponds. The total study area that is part of the creek shed comprises a 4 $km^2$ catchment that is over 80% impervious with the large concentration of impervious surfaces located near the centroid of the watershed. The catchment is comprised of 11 storage basins, ranging in volume from 370 m$^3$ to 32000 m$^3$.The land types of this study case include residential areas with 15% of total area, commercial areas with 55% of total area, and industrial areas with 30% of the total area. Annual precipitation is about 2.50 meters, including approximately 1.45 meters of snowfall. The climate in the study area is classified as humid continental with severe winters, hot summers, no dry season, and strong seasonality. The current stormwater system design standard for the urban drainage Network A has a 10% annual exceedance probability, 12-hour storm. This storm is 73.66 millimeters of rainfall using NOAA Atlas 14 rainfall volumes. One reason to choose this modeled drainage network is that there is low baseflow with fewer groundwater effects. This condition offers less interference for the simulating control strategy of flooding mitigation (HRWC, 2013). Another motivation in selecting this case study is that it has been previously retrofitted with wireless sensors and control valves (Bartos et al., 2018). This retrofitted urban watershed will serve as a real-world testbed for the modeling outcomes in this paper. At the current stage, this catchment has ongoing efforts to reduce erosion and alleviate flooding conditions.

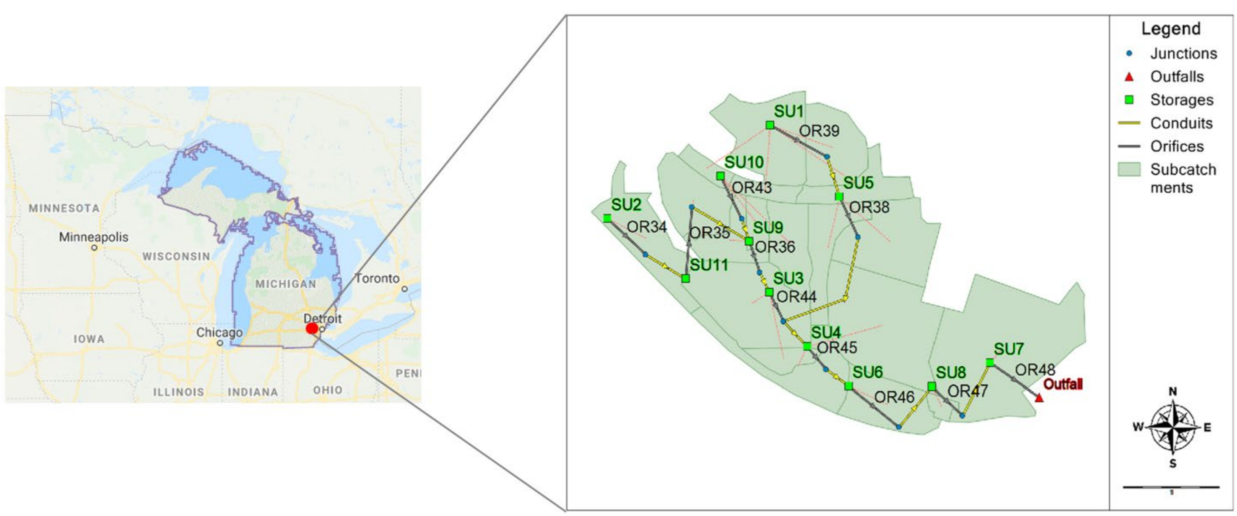

Fig.1. The study urban watershed is located in the southeast of Michigan state, U.S., ( left plot: red point is the location of study case) and the topological view of the SWMM model (Network A), plotted by using PCSWMM v.7.2. (right plot: scale unit is kilometer; yellow label for storage unit ID; green label for orifice ID).

## 2.2 Co-simulating Rainfall-runoff and Control Model

### 2.2.1 Hydraulic Module

The hydraulic-hydrologic model, called Network A, was established based on the US Environmental Protection Agency SWMM (Storm Water Management Model) (Rossman, 2015). This SWMM model has been calibrated and validated, results showing that the differences between simulated and measured volume and flow are generally within 15% and 20% respectively (SMITH, 2015). The Network A SWMM model used a non-linear reservoir schematization, manning's equation, dynamic wave routing model, and the Green-Ampt infiltration model for surface runoff and the full Saint Venant equations for flow routing in conduit systems. The simulation timestep for this study was set to 5 minutes. This SWMM model, including the controlled stormwater basin and its pipeline system, This SWMM model, including the controlled stormwater basin and its pipeline system, simulated 0.1 $m^2$ circular orifices as gates, which are located at the bottom of the storage node. Each orifice had a higher invert elevation than the overflow height of all downstream storage nodes and all conduits between storage nodes were circular in geometry with length in ranges from 40 m to 400 m and Manning roughness coefficient of 0.01.These gates can be adjusted automatically during each simulation step. There are a total of 11 storage units (green square of Fig.1) labeled 'SU' on the basins (green labels of Fig.1) and 11 orifices (yellow link of Fig.1) labeled 'OR' (yellow labels of Fig.1). The orifices are physically connected with storage facilities and receive orders from storage units before taking action.

### 2.2.2 Water Quality Module

In this case study, a water quality model composed of pollutant buildup, wash off, routing, and reaction procedures were built. The water quality model is not calibrated or validated due to the limited availability of water quality measurements. Thus, the water quality results are only for evaluating control scenarios, and not for making absolute, quantitative predictions or comparing with simulations from other water quality models. The water quality simulation considers Total Suspended Solids (TSS) as the pollutant of interest. To model TSS, four steps including the build-up, wash-off, routing, and reaction are simulated by SWMM software. For each stage, the processes of build-up and wash-off happen on the land surface while the procedure of TSS routing and reaction occurs in conduit. The conduits and storage nodes are assumed to behave as a continuously stirred tank reactor where the outflow concentration is equal to the concentration in the CSTR in equation 3. Different functions are created below to represent how TSS modeling is performed in SWMM. The removal mechanism for TSS is modeled as first-order decay, which is determined by the settling velocity of the suspended solids. For the TSS build-up, the exponential function was shown in equation 1 (Alley, 1981).

$$B_{(t)} = C_1 \times (1 - \mathrm{e}^{-(C_2 \times \mathrm{t})}) \quad (1)$$

Where $B_{(t)}$ is accumulated TSS buildup amount at time t over the sub-catchments' land-use area [mg/ L]; $C_1$ and $C_2$ are build-up parameters in exponential function; $C_1$ is the maximum possible build-up normalizer, and in this case, was set to be area; $C_2$ is a scaling factor which is a multiplier used to adjust the build-up rates listed in the time series.

For the TSS wash-off, the Event Means Concentration (EMC) function, which is a special case of Rating Curve Wash-off equation (2) where the exponent $C_2$ is 1.0 and the coefficient $C_1$ represents the wash-off pollutant concentration in mass per liter, was adopted to calculate this amount in equation 2, below.

$$W_{(t)} = C_1 \times Q^{C_2} \tag{2}$$

Where $W_{(t)}$ is accumulated TSS wash-off amount at the time [t] over the sub-catchments' land-use area [mg/ L]; Q is runoff rate [mm/ hour]; $C_1$ represents the washoff pollutant concentration [mg/ L]; $C_2$ is the exponent, equal to 1.0.

However, there are no standard criteria for establishing the buildup and wash-off function, or no universal parameter values can be used for pollutant and land-use specific cases. According to nation-wide datasets, this study determines representative estimates of parameter values of the build-up and wash-off model (Sullivan et al., 1977). A summary of assigning parameters was listed in table 1.

Table 1 Parameter Setting of Build-up and Wash-off Model

| Model / Parameter / Land Type | Build-up Model | | Wash-off Model | |
|---|---|---|---|---|
| | C1 | C2 | C1 | C2 |
| Commercial Use | 12 | 5 | 25 | 1 |
| Industrial Use | 27 | 0.5 | 21 | 1 |
| Residential Use | 21 | 0.3 | 29 | 1 |

To simulate the TSS transportation, the concentration of TSS exiting the conduit at the end of a time step is calculated by integrating the conservation of mass equation (3), using average values for quantities that might change over the time step such as flow rate and conduit volume (Sullivan et al., 1977). In this way, there is no need to compute the spatial variation of concentration along the length of a conduit.

$$\frac{d(Vc)}{dt} = C_{in}\, Q_{in} - cQ_{out} - cK_1 \quad (3)$$

where V is the volume within the reactor [L], c is the concentration within the reactor [mg/ L], $C_{in}$ is the concentration of any inflow to the reactor [mg/ L], $Q_{in}$ is the volumetric flow rate of this inflow [L/s], $Q_{out}$ is the volumetric flow rate leaving the reactor [L/s], and $K_1$ is a first-order reaction constant.

For the TSS reaction, the links and nodes are assumed as completely mixed reactors, and a first-order reaction equation was formulated to calculate the concentration of TSS at a given time in equation 4 below.

$$M_t = M_0 e^{-kt} \quad (4)$$

Where $M_t$ has accumulated TSS concentration at time [t] over the sub-catchments' land-use area [mg/ L]; $M_0$ is the initial TSS concentration at time [t]; k is the constant first-order reaction rate constant for TSS [1/t]; t is the current reaction time.

### 2.2.3 Control Module

PySWMM is a Python language software package for the creation, manipulation, and study of the structure, dynamics, and function of complex drainage networks (McDonnell et al.,2017). PySWMM can be used to streamline stormwater modeling optimization and control-processing. This allows the control rule to be designed and implemented outside of the original SWMM model, which enables control algorithms to be developed exclusively in Python with the use of functions and objects as well as storing and tracking hydraulic trends for control actions (Sadler et al., 2019a). However, the existing official PySWMM version does not have 'setter' and 'getter' functions for generating the time-series output of water quality simulation at the current stage. It is still unlikely to obtain the nodes' and links' pollutant concentrations at each co-simulation step. To solve this problem, the water quality modeling functions were added to PySWMM by replacing a new library module (Sharior et al., 2019). This compiler allows PySWMM to extract time-series pollutant concentrations at junctions.

## 2.3 Rainfall Datasets

### 2.3.1 Measured Rainfall Data

The rainfall measurements for controller performance assessment were gathered from the 'Big House Station' of the Weather Underground. This station is close to the study catchment, and it has 15-minute resolution rainfall measurements starting in 2007, which have been disaggregated into the 5-minute interval. Three-day rainfall measurements with 82.81 millimeters total rainfall volume from 07/05/2014 to 07/07/2014 were imported into .inp file as rainfall inputs for rainfall-runoff simulation.

### 2.3.2 Artificial Rainfall Data

In the controller site selection process, a total of 9 artificially-designed short-duration rainfall events were used to assess the performance of selected controllers in Fig.2. During each rainfall event, the correlation between the water depth and the orifice setting was quantified. These short-duration rainfall events with 5-minute intervals are distributed by the Chicago rainfall pattern, which was commonly used for calculating approximate rainfall-runoff and constructing the runoff hydrograph (NRCS, 1986).

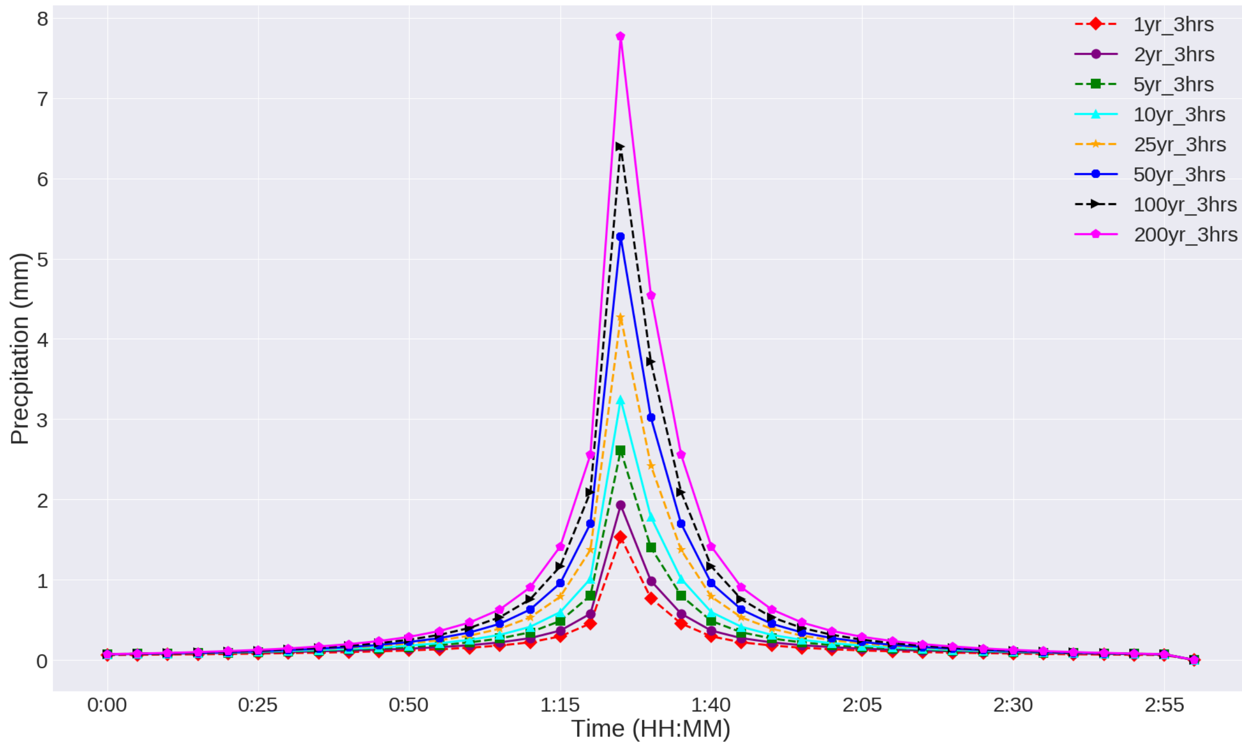


Fig.2. 8 Artificially Designed Rainfalls for SWMM (Storm Water Management Model) Simulation, 'yr' representing the number of year and 'hrs' standing for hours.

# 3. Methodology

In this work, four control scenarios abbreviated as 'Baseline,' 'Downstream,' 'Sys_S,' and 'Sys_D' were conducted to analyze the controller performance and controller placement. This analysis was carried out within three steps. In the first step, a rainfall-runoff model that was assembled with hydraulics and water quality routing procedures were developed. Running this model, the second simulates those four control scenarios, which facilitates the coordination of the control strategy. Finally, the controller performance in eliminating flooding and total suspended solids load were assessed, and the suitable controller sites were suggested as well.

## 3.1 Control Scenarios

### 3.1.1 Control Rules and Controllers

The controller in this paper can be considered as a conceptual function to characterize the relationship between storage water depth and orifice setting, while the storage unit is physically storage structure such as ponds (Shishegar et al., 2019; Wong and Kerkez, 2018). In this study, the pre-defined multi-linear mathematical correlation between water depth and orifice setting was refined, and the baseline water depth (BD), threshold water depth (TD), and maximum water depth (MD) are set according to the suggestions from Mullapudi et al., 2018. These controllers are used to determine the opening percentage of orifices at a 5-minute time step during rainfall events. The control rules are set to reflect the controller's logic. These rules are:

Rule 1: If a rainfall event comes, close the sluice gate and store the water to minimize the most downstream flooding stress although it is still raining.

Rule 2: If the water depth of the pond (storage unit) reaches the predefined Baseline water Depth (BD), keep closing the sluice gate until there is an upward trend of flooding duration at downstream nodes.

Rule 3: If the water depth of the pond is over the real Threshold water Depth (TD), partially open the sluice gate to prevent overflow.

Rule 4: If the water depth of the pond is over the predefined Maximal water Depth (MD), completely open the sluice gate to limit the flooding effects on the entire system.

Rule 5: If the water depth of the pond is controlled between BD and TD, and also the runoff is continuing, gradually open the sluice gate to adapt to the water coming and releasing.

Rule 6: If the water depth of the pond is controlled between the threshold and maximal water depth and the runoff is continuing, adjust the sluice gate opening at a system-level scale to reduce the nodal flooded hours.

### 3.1.2 Control simulations

Four types of control scenario simulations are performed under a two-day hydrologic-hydraulic modeling process with rainfall events. These four control scenarios are designed by control setting, control objects, actuators, and targeting location. Control setting means control strategy. For instance, the 'Baseline' control scenario means no control applied. The control object is equal to the storage unit being controlled. Actuators are the same as the orifices, while the targeting location is the elements of interest. A summary of the scenarios design can be checked in Table 2.

Table 2 Control Scenario Design

| Control Scenarios | Control Setting | Controlled Objects | Actuators | Targeting Location |
|---|---|---|---|---|
| Baseline control | without control | none | none | downstream flooded nodes and all storage units |
| Downstream control | only one single controller implemented at the most downstream site | the most downstream storage unit (SU7) | downstream orifice (OR48) | downstream flooded nodes: J18, J24, J25, and J26 |
| 'Sys_S' control | system-level control with 11 same controllers | all storage units | all orifices | downstream flooded nodes and all storage units |
| 'Sys_D' control | system-level control with 11 different controllers | all storage units | all orifices | downstream flooded nodes and all storage units |

The descriptions for each control strategy can be found below:

1. Baseline without control ('Baseline' as an abbreviation): of this scenario, there are no controller actions, and orifices keep open. All controllers follow rule 1 to generate the original states of nodes, conduits, and storage units.

2.The most downstream control ('Downstream' as an abbreviation): Downstream control is defined to solely control the most downstream sluice gate for minimizing the most downstream flooding and TSS. In this way, this scenario follows rules 1, 2, 3, and 5. In this single one controller, the baseline water depth (BD), threshold water depth (TD), and maximum water depth (MD) are set to be 0.78 meters, 2 meters, and 2.64 meters, respectively.

3.System-level control with 11 same controllers ('Sys_S' as an abbreviation): 'Sys_S' means using 11 of the same controllers to adjust the corresponding orifices. Therefore, a blanket operation rule will be applied to all tanks simultaneously during a storm. At a system-level scale, the interactions between different storage units should be taken into consideration for improving the whole system's operation efficiency at the global angle. Therefore, all rules, except rule 6, are considered in this simulation scenario. Those ponds are controlled with 11 sluice gates following the same control strategy.

4.System-level control with 11 different controllers ('Sys_D' as an abbreviation): 'Sys_D' is to consider 11 different controllers, where 11 various rule settings are used to regulate orifices. Different from scenario 3, this scenario was set to explore suitable water depth settings for multiple controllers and not just one controller. In this scenario, the BD, TD, and MD are fixed, and then simulations are performed to simultaneously update the controller's water depth setting until rule 6 was achieved. All rules applied in control scenarios were shown in table 3, and the final controller setting was presented in table 4. In table 3, each control scenario was composed of different control rules. Using the 'Sys_S' scenario as an example, this control strategy was conducted by applying rule 1, rule 2, rule 3. Rule 4 and 5 to simulation. Table 4 presented the ultimate correlation between Actual water Depth (AD) and the orifice setting, which was utilized for defining the controller.

Table 3 Combinations of Control Scenarios and Rules

| Control Scenarios | Rule 1 | Rule 2 | Rule 3 | Rule 4 | Rule 5 | Rule 6 |
|---|---|---|---|---|---|---|
| Baseline | + | | | | | |
| Downstream | + | + | + | | + | |
| Sys_S | + | + | + | + | + | |
| Sys_D | + | + | + | + | + | + |

Table 4 Relationship between Water Depth and Orifice Setting

| Controller ID | Storage Unit ID | Orifice ID | BD/meter | TD/ meter | MD/ meter | Orifice Setting |
|---|---|---|---|---|---|---|
| 1 | SU1 | OR39 | 0.78 | 2.00 | 2.91 | If AD<BD, close gate to 100%;<br>If BD<AD<TD, open gate to 25%;<br>If TD<AD<MD, Open gate to 75%;<br>If AD>MD, open gate to 100%. |
| 2 | SU2 | OR34 | 0.78 | 2.30 | 2.91 | |
| 3 | SU3 | OR44 | 0.78 | 2.00 | 2.91 | |
| 4 | SU4 | OR45 | 0.78 | 2.30 | 2.76 | |
| 5 | SU5 | OR38 | 0.78 | 2.00 | 2.47 | |
| 6 | SU6 | OR46 | 0.78 | 2.00 | 2.47 | |
| 7 | SU7 | OR48 | 0.10 | 2.00 | 2.76 | |
| 8 | SU8 | OR47 | 0.78 | 2.00 | 2.61 | |
| 9 | SU9 | OR36 | 0.78 | 2.00 | 2.61 | |
| 10 | SU10 | OR43 | 0.78 | 2.00 | 2.47 | |
| 11 | SU11 | OR35 | 1.39 | 2.00 | 2.47 | |

## 3.2 Controller Performance Evaluation

As a control logic in the urban drainage systems, the real-time controller is required to have a good performance in terms of keeping the peak water depth below the threshold line during the peak rainfall period. Each storage unit can remove the coming pollutant, and, at the same time, reduce the flooding duration to a certain level. Therefore, three indicators of real-time controller performance are proposed below, and each of them is set to meet the requirements of this control logic.

### 3.2.1 Peak Depth Shaving Efficiency

The first indicator for evaluating the real-time controller performance is set to reduce the peak depth of upstream storage units. In this paper, the term 'Peak Depth Shaving Efficiency' in equation 5 was proposed to represent the first metric, which is abbreviated as PDSE.

$$PDSE_{[i]} = \left(\frac{Peak\ Depth_{[i,b]} - Peak\ Depth_{[i,c]}}{Peak\ Depth_{[i,b]}}\right) \times 100\% \quad (5)$$

Where Peak Depth Shaving Efficiency$_{[i]}$ is the peak water depth shaving efficiency for the ith storage unit fraction [%]; Peak Depth$_{[i,b]}$ is the peak water depth for the ith storage unit under baseline simulation scenario [meter]; Peak Depth$_{[i,c]}$ is the peak water depth for the ith storage unit under control simulation scenario [meter].

### 3.2.2 Pollutant Removal Efficiency

The second indicator for assessing the real-time controller performance is set to quantify the capability to remove total suspended solids of upstream storage units. To that end, a term called 'Pollutant Removal Efficiency' (PRE) was put forward in equation 6.

$$PRE_{[i]} = \left(\frac{TSS_{[i,b]} - TSS_{[i,c]}}{TSS_{[i,b]}}\right) \times 100\% \quad (6)$$

Where $PRE_{[i]}$ is the pollutant removal efficiency for the ith orifice fraction [%]; $TSS_{[i,b]}$ is the load of TSS (Total Suspended Solids) for the ith orifice under the baseline simulation scenario [kg]; $TSS_{[i,c]}$ is the load of TSS for the ith orifice under control simulation scenario [kg].

#### 3.2.3 Flooded-hour Reduction

This study adopted Flooded-hour Reduction, called FR, as the third performance indicator. The third indicator was set to evaluate the real-time controllers' performance in flooding mitigation. Equation 7 was established to alleviate the flooding duration of downstream flooded nodes.

$$FR_{[i]} = Flooded\ Hour_{[i,b]} - Flooded\ Hour_{[i,c]} \quad (7)$$

Where $FR_{[i]}$ is the Flooded-hour Reduction for the ith flooded node [hour]; $FR_{[i,b]}$ is the Flooded-hour Reduction of the ith flooded node under baseline simulation scenario [hour]; $FR_{[i,c]}$ is the Flooded-hour Reduction of the ith flooded node under control simulation scenario [hour].

### 3.3 Controller Site Selection

Different from the 'Downstream' control, system-level control ('Sys_S' and 'Sys_D') allows several controllers to be simultaneously operated at a system-scale during the storm event. Rather than solely applying a blanket rule to the most downstream controller on the 'Downstream' scenario, system-level control has the potential to offset the timing of the flood peaks from different sub-catchments. However, one disadvantage of placing distributed controllers to regulate hydraulic and water quality features is that some of the controllers might worsen the system performance by generating adverse influences, finally pushing the stormwater system to be away from the desired outcomes(Emerson et al., 2005). Thus, it is of great importance to identify the site candidate for controllers with a positive performance and remove the controllers who have disadvantageous impacts on the system response. Controllers are likely to shave the upstream peak water depth in the sacrifice of triggering downstream flooding and TSS loading. The controller placement should achieve global benefits while single index consideration might not be the advantage of the system-level control. For this purpose, one metric called Controller Placement Index (CPI) was defined as the indicator for controller placement identification under artificially-designed rainfall events. CPI was formulated by adding PDSE, PRE, and FR with different weighting factor shown in Equation (8).

$$\mathrm{CPI} = PDSE_{[j]} \times w1 + PRE_{[j]} \times w2 + FR_{[j]} \times w3 \tag{8}$$

Where $CPI_{[j]}$ is the value of Controller Placement Index for the jth controller; $PDSE_{[j]}$ is the peak water depth shaving efficiency of corresponding the jth storage unit 'Sys_D; $PRE_{[j]}$ is the pollutant removal efficiency of the jth storage unit under 'Sys_D' control simulation scenario; $FR_{[j]}$ is the flooded-hour reduction for the flooded node right after the jth storage unit the under 'Sys_D' control simulation scenario. For instance, the junction J18 is right after SU1, so we consider the FR value of J18 as FR1. w1, w2, and w3 are the weighting factors for index PDSE, PRE, and FR, respectively. In this study, these values (0.4 for w1, 0.3 for w2, and 0.3 for w3) for weighting factors were determined by the experimental modeling trials (Li et al., 2019a). Of this part, 9 short-duration rainfall events with different return periods are simulated to evaluate controller placement by using CPI.

# 4. Results and Discussions

## 4.1 Time-series Control Settings

Compared with the traditional SWMM, PySWMM has a crux advantage in displaying the control settings at step-by-step style. As mentioned in (2.3) of the methodology section, the open percentage dynamically adjusts itself based on the pre-set control rules for each orifice. These actions taken by orifice OR48 are helpful for discovering the pattern of continuous orifice settings at a step-wise simulation procedure. A typical example to account for the continuous orifice open/close status is the open percentage time-series plot.

Fig.3 shows that smaller orifice settings in orifice OR48 appear on the 'Downstream' and 'Sys_S' control scenarios. Although the 'Sys_D' control scenario shows a similar changing pattern, orifice settings of the 'Sys_D' control scenario are relatively larger at each timestep. Less fluctuation in orifice settings requires less energy for actuator operation, indicating the control system is more stable. Such gentle and steady operation in orifice is beneficial for avoiding abrupt actions and sudden movements of the outlet gate in practice. Although the orifice setting fluctuation of the 'Sys_D' is more significant than the other two scenarios, the time when orifice setting fluctuates up-to-down is earlier at 'Sys_D' than the other two scenarios (Fig.3). The fluctuation in the 'Sys_D' scenario requires more energy, for instance, electricity supply, to operate it in real situations where system instability may be magnified at this point. Thus, it can be inferred that 'Sys_D' is more likely to result in wear on actuators.

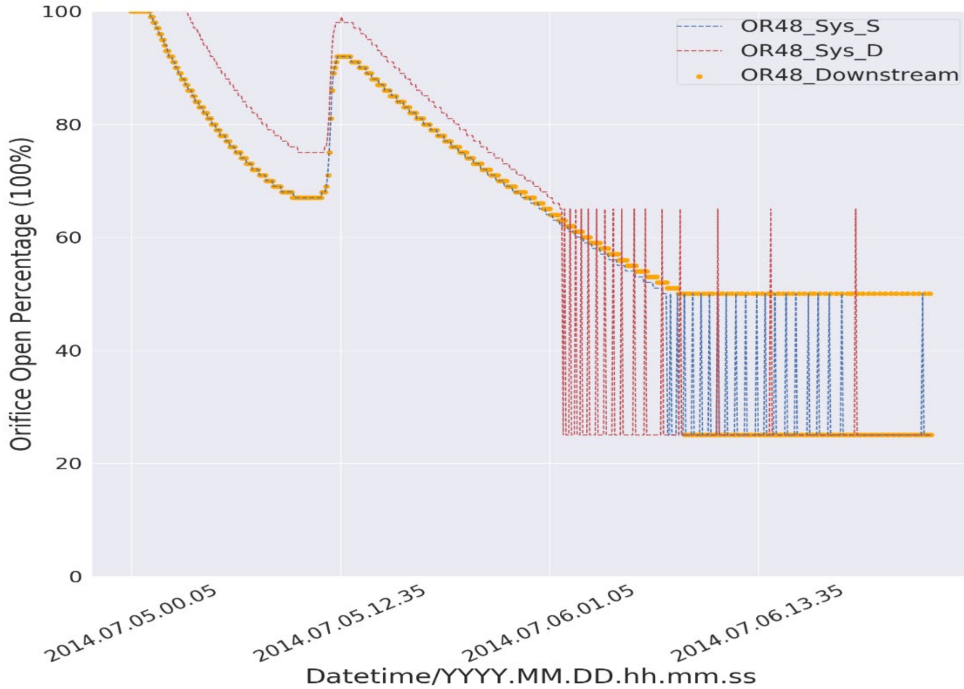


Fig.3. Time-series Plot of the Actions taken by Orifice OR48 (Orifice Settings) on control scenarios: the most downstream control scenario (‘Downstream’, yellow scatter), system-level control scenario with 11 same controllers (‘Sys_S’, blue dashed line) , system-level control scenario with 11 different controllers (‘Sys_D’, red dashed line).

Despite the time-series plot differences in Fig.3, PySWMM takes full advantage of storing and tracking the control actions. This offers researchers a precedent opportunity to gain an insight into how orifices adapt to the water quantity and quality changes. By better understanding how each orifice is adjusted, the setpoints for water quantity and quality, such as flow and total suspend sedimentation can be reached with minimal fluctuations.

### 4.2 Simulated Water Quality Outcomes

With PySWMM, SWMM water quantity and quality modules can be loaded and executed in a stepwise fashion. Afterward, the modeled hydraulic states can be extracted, but the water quality information is not available for access. This is because the current PySWMM version doesn’t have the functionality to obtain simulated water quality data. This study tested the PySWMM tool by running water quality functions. By doing this, the time-series water quality results can be visualized in a statistical plot.

Fig.4 shows the boxplots for simulated time-series TSS concentration under different control scenarios. Surprisingly, only the TSS concentration of SU4 (highlighted by red dash square) and SU7 (highlighted by green dash square) changed under different control scenarios while others remain constant. This result is in line with the finding that the effectiveness of RTC strategy is related to the pond storage volume (Shishegar et al., 2019). Taking a closer look, we can notice that the TSS concentration of SU4 reduced much more than SU7. As noted in the 'Study Area' section, SU4 is the storage unit with the highest structural depth and the largest volume, which creates a substantially longer detention time than other storage units. This can be one potential explanation for making the TSS concentration of SU4 decline more apparently than SU7 when 'Sys_S' and 'Sys_D' control was applied. Different from SU4, SU7 is the most downstream storage unit. The location of SU7 allows it to be the furthest structure to release water into a receiving water body, resulting in a longer detention time as well. Overall, the decrease of TSS at SU4 and SU7 can be attributed to the increase of detention time during the modeling steps (Carpenter et al., 2014).

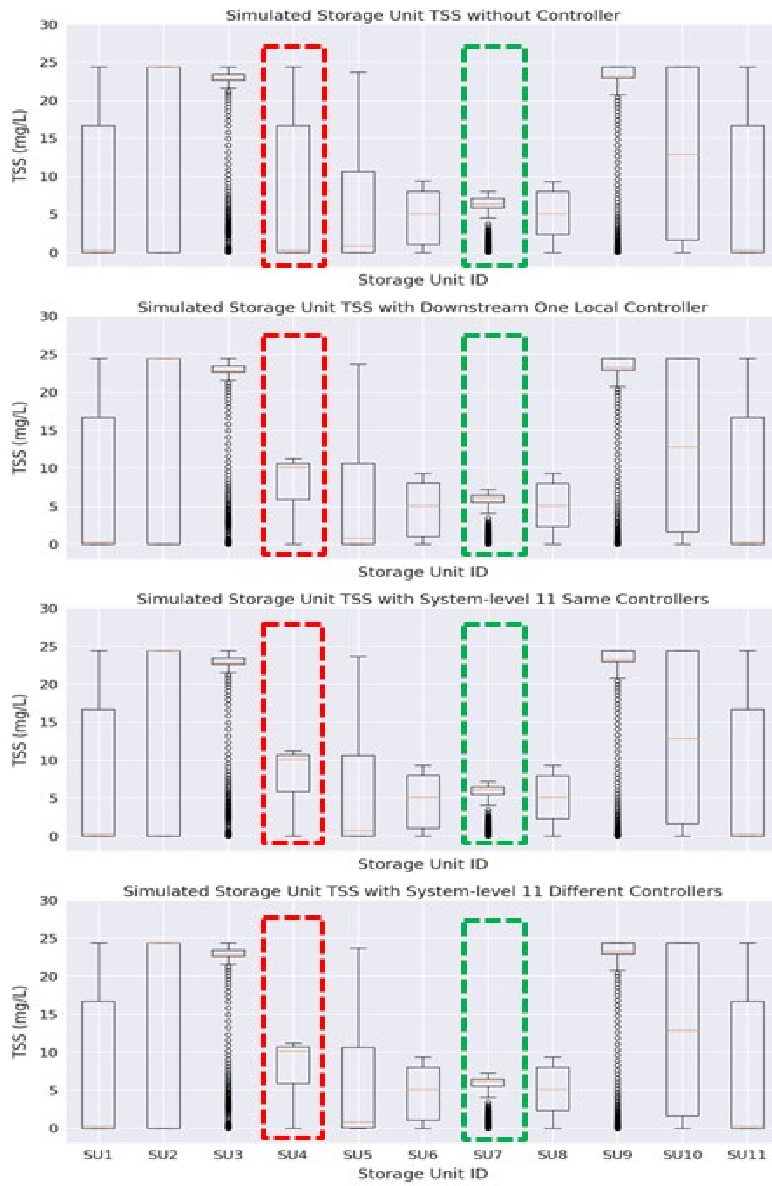


Fig.4. Boxplot of Total suspended solids (TSS) concentration at the storage units under no control ('Baseline', the first boxplot), the most downstream control ('Downstream', the second boxplot), system-level control with 11 same controller ('Sys_S', the third boxplot), and system-level control with 11 different controllers ('Sys_D', the fourth boxplot).

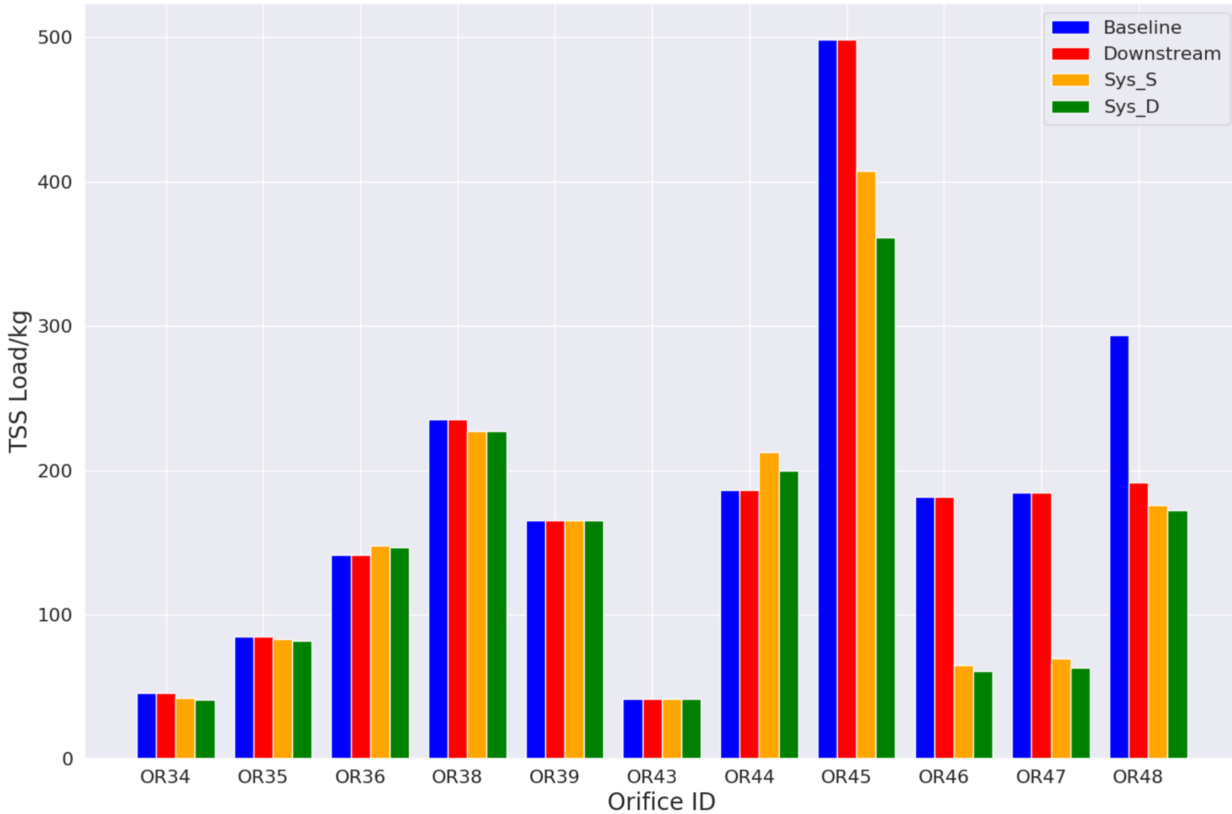


Fig.5. Barplot of Total suspended solids (TSS) load at orifices for cases with no control scenario ('Baseline'), the most downstream control scenario ('Downstream'), system-level control scenario with 11 same controllers ('Sys_S' ) , system-level control scenario with 11 different controllers ('Sys_D'), and eleven controllers operated in coordination by these control strategies.

In spite of limited effects on SU's TSS concentration, Fig.5 presented that these two system-level control scenarios ('Sys_S' and 'Sys_D') have reduced the TSS load. As we can see, the amount of the TSS load under 'Downstream' control remains same as that of the TSS load under baseline scenario. However, there is about 113.40kgs TSS dropped at the most downstream orifice OR48. Notwithstanding the evidence, over half of the orifices' TSS loading decreased when 'Sys_S' or Sys_D' control was implemented. It can be observed that the TSS loading of downstream orifices like OR45, OR46, OR47, and OR48 noticeably declined; the reduction magnitude of TSS loading on 'Sys_D' (with minimum 120.83 kgs and maximum 137.39 kgs) is larger than that on 'Sys_S' scenario (with minimum 91.39 kgs and maximum 117.63 kgs). These results present an implication that ‘Sys_D’ control should be more capable to alleviate pollutant stress than ‘Sys_S’ and ‘Downstream’ control. Taking the system remaining TSS loads into account (Fig.6), the outfall produced the biggest TSS decrease with 41.36% under ‘Sys_D,’ followed by ‘Sys_S’ with 40.08% TSS reduction while the ‘Downstream’ control had the least TSS decline percentage with only 34.71%. Therefore, ‘Sys_D’ appears to be the best control scenario to maximize the benefits of pollutant removal, but the controller performance in this regard still needs testing under synthetic rainfalls (Sharior et al., 2019; Shishegar et al., 2019).

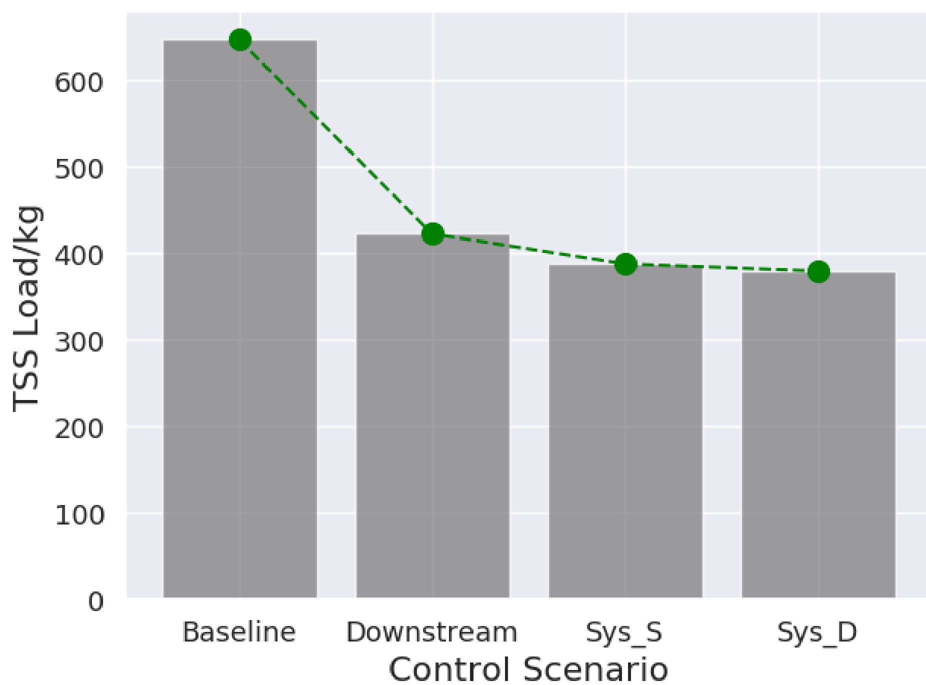


Fig.6. Barplot of Total suspended solids (TSS) load at Outfall under three control scenarios including the no control (‘Baseline’ scenario), the most downstream control (‘Downstream’ scenario), system-level control with 11 same controllers (‘Sys_S’ scenario), and system-level control with 11 different controllers scenario (‘Sys_D’ scenario).

## 4.3 Controller Performance Evaluation

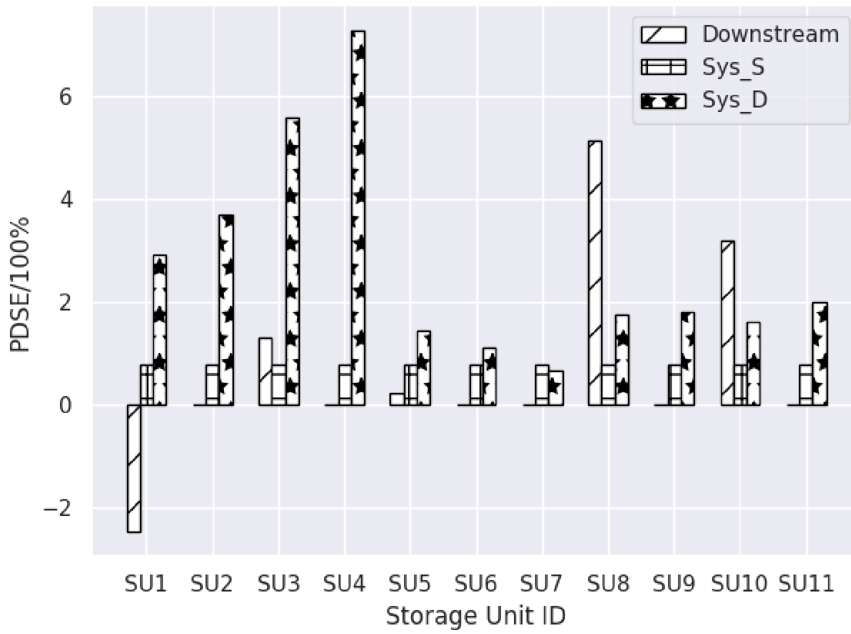


(a)

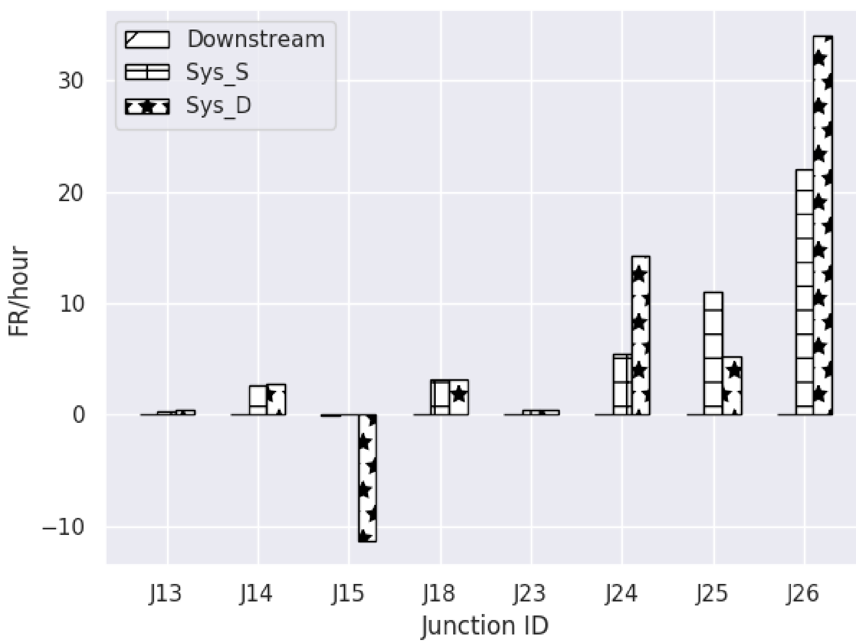


(b)

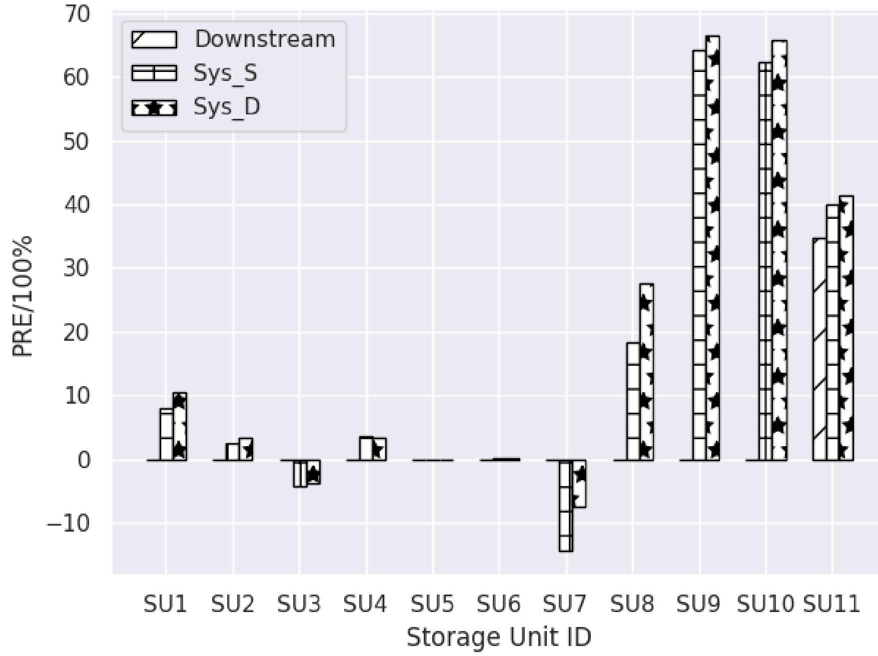


(c)

Fig.7. Comparisons of (a) Peak Depth Shaving Efficiency (PDSE), (b) Flooded-hour Reduction (FR), (c) Pollutant Removal Efficiency (PRE) under Three Control Scenarios including the no control ('Baseline' scenario), the most downstream control ('Downstream' scenario), system-level control with 11 same controllers ('Sys_S' scenario), and system-level control with 11 different controllers scenario ('Sys_D' scenario).

In this study, the comparisons between PDSE, PRE, and FR were used to evaluate the controller performance under different control scenarios. Fig.7a shows that the largest PDSE was from the 'Sys_D' case, where PDSE went up to 7.30% at SU4. Conversely, the biggest PDSE at SU8 (5.13%) and SU10 (3.20%) comes from the scenario of 'Downstream'. This difference reveals that the most downstream controller has better behavior in improving the most downstream PDSE. The evidence from the PDSE comparison implies that the 'Downstream' control strategy has more ability to reduce the most downstream hydraulic stress.

A total number of 8 junctions (J13, J15, J18, J23, J24, J25, J26) of the SWMM model are flooded under the two-day rainfall-runoff simulation. FR (Flooded-hour Reduction) was employed to quantify the RTC capability of mitigating downstream flooding. Fig.7b demonstrates that controllers implemented at 'Sys_S' and 'Sys_D' strategy have significant FR value at downstream nodes such as J24, J25, and J26. However, those controllers pose limited effects on FR on the 'Downstream' scenario. Although the flooding duration slightly decreases at upstream nodes including J13, J15, and J18, flooded hour reductions are not notable in these junctions. Fig.6b shows that the largest FR is still below 5 hours in most of the upstream junctions (J13, J14, J18, and J23). The largest flooding hour reduction happens at J25, where the FR value (34.08 hours) of the 'Sys_D' scenario is 54.84% higher than that (22.01 hours) of the 'Sys_S' scenario. As we discussed, system-level control is a trade-off between upstream storage capacity and downstream flooding mitigation. For example, if there is extreme rainfall, basically, the gate would be closed and water of the pond will slowly be discharged into the downstream flooded locations. However, if the gate is closed too much or too long, there will be overflow issues in upstream ponds. In Fig.9 a, b, and c, we can found there are some negative values (abnormalities). For instance, Fig.9 b shows that J15 has negative flooding hour reduction in the 'sys_D' scenario. This means system-level control has increased the flooding duration in junction J15. This can be attributed to the opening of the gate too much or too long, and then, leading to downstream local flooding issues. The FR analysis above summarizes that the distributed system-level control outperforms individual downstream control in terms of tackling flooding issues.

With regard to TSS removal, Fig.7c shows there are fewer PRE value differences between 'Sys_S' and 'Sys_D' situation. A positive PRE over 60% was found at 'Sys_S' and 'Sys_D' scenarios, which agreed with the outcomes (Gaborit et al., 2016, 2013). In the 'Downstream' scenario, most of the storage units' PRE values are below 10%. The only PRE value that reached a comparable level (40% FRE) was generated by the 'Downstream' controlled storage unit SU48, which is located at most downstream sites. This can be inferred that the local controller has the possibility to behave as those system-level controllers did concerning water quality improvement at downstream locations.

In summary, a majority of the controllers on the 'Sys_D' scenario realized the goals of promoting PDSE, FR, and PRE more or less during the typical two-day rainfall event. Controllers on the scenario of 'Sys_D' outperform the other two regarding flooding mitigation and pollutant removal. Our results illustrate that global benefits can be obtained by system-level control, although it requires more operation energy. Moreover, this work used two-day long rainfall measurements as the simulation inputs and assessed the controller performance during this 48-hour rainfall-runoff simulation. However, the impacts of rainfall variability on controller performance were not explored in this study. Rainfalls with different intensities can be utilized to investigate the performance of real-time control for addressing water quantity and quality problems.

## 4.4 Controller Site Selection

Prior work has documented the controller site selection by ranking the system-wide performance improvement to determine the best candidate sites for the controller and increasing the number of controlled storage units to gain the most prominent benefits (Wong, 2017). For example, it was found that when the control network was deployed through 10 or more controllers, the system-level benefits would decay. However, the assessment of the controller placement for pollutant removal efficiency was seldom considered under various rainfall scenarios. This study adopted the CPI (Controller Placement Index) to select the controller site under a range of artificially designed rainfalls.

Fig.8 implies that controller 1 and 8 outperformed controller 4 and 6 in the majority of rainfall scenarios. With the basis of Figure 8(d), it was evident that controller 1 and controller 8 displayed a considerably higher CPI value than controller 4 and controller 6. This evidence depicts that controller 1 has more abilities to adapt to rainfall changes with the highest CPI 0.377 and lowest CPI 0.0081, all higher than others. As detailed in Fig.8 a, b, and c, the components of CPI (PDSE, FR, and PRE) of controller 1 and 8 show an apparent growth when compared with controller 4 and 6. Controllers 1 and 8 are more likely to balance PDSE, FR, and PRE in an adaptive way than the other 2 controllers. One unusual scenario is that, under extreme rainfall events (100year-3hours and 200year-3hours), controller 8 reported similar PDSE, FR, and PRE to controller 4 and 6. The negative CPI values in control 4 (-0.012 under 20 year-3 hours and -0.047 under 25 years-3 hours) and controller 6 (-0.039 under 20 year-3 hours and -0.079 under 25 years-3 hours) reduced scores for site selection by leading to marginal effects. The representations in Fig.7 indicate that controller 1 and controller 8 are more capable to withstand higher intensity rainfall scenarios and to adapt to different rainfall pattern changes. The CPI values are in accordance with the statements that real-time control should be flexibly adaptive to environmental changes. It is necessary to make the controller placement increase its adaptability. The findings above extend the controller site evaluation requirements, demonstrating that CPI can help filter those controllers with unfavorable performance under intensive storm scenarios.

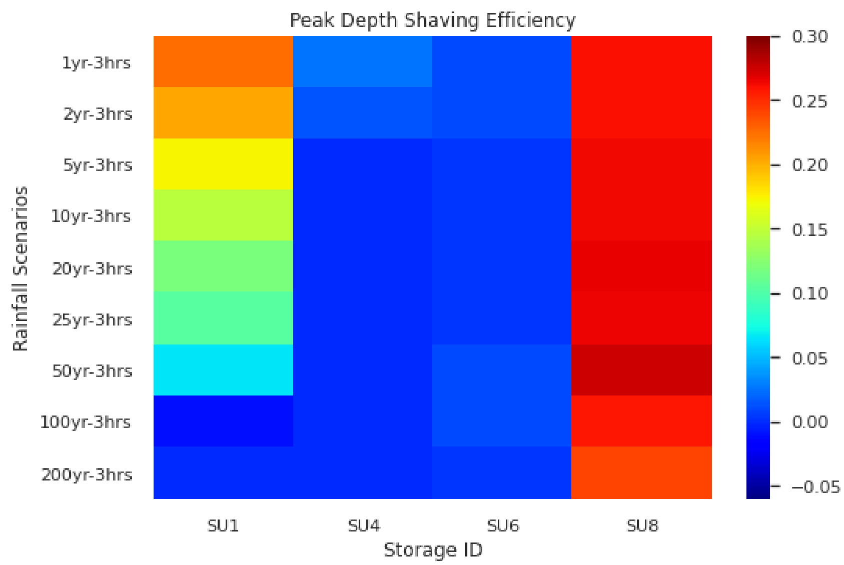
Peak Depth Shaving Efficiency
Rainfall Scenarios
1yr-3hrs
2yr-3hrs
5yr-3hrs
10yr-3hrs
20yr-3hrs
25yr-3hrs
50yr-3hrs
100yr-3hrs
200yr-3hrs
SU1
SU4
SU6
SU8
Storage ID
0.30
0.25
0.20
0.15
0.10
0.05
0.00
−0.05

(a)

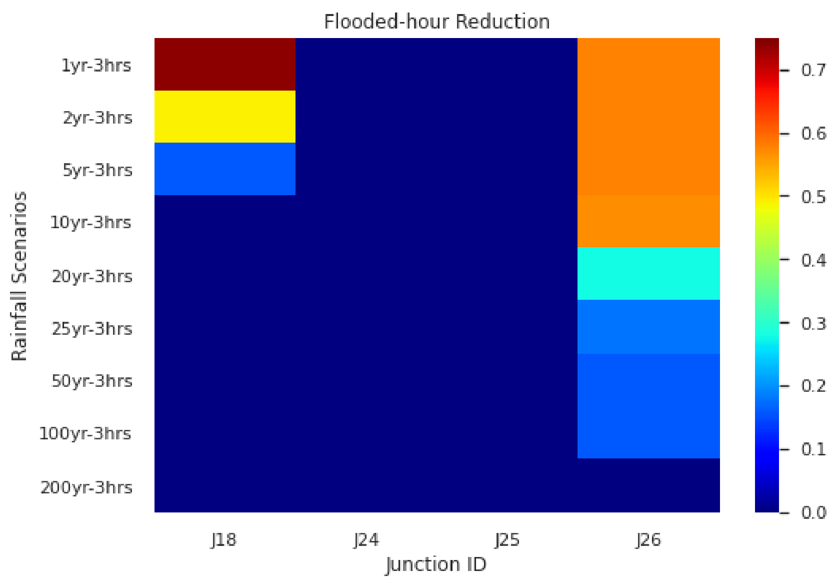
Flooded-hour Reduction
Rainfall Scenarios
1yr-3hrs
2yr-3hrs
5yr-3hrs
10yr-3hrs
20yr-3hrs
25yr-3hrs
50yr-3hrs
100yr-3hrs
200yr-3hrs
J18
J24
J25
J26
Junction ID
0.7
0.6
0.5
0.4
0.3
0.2
0.1
0.0

(b)

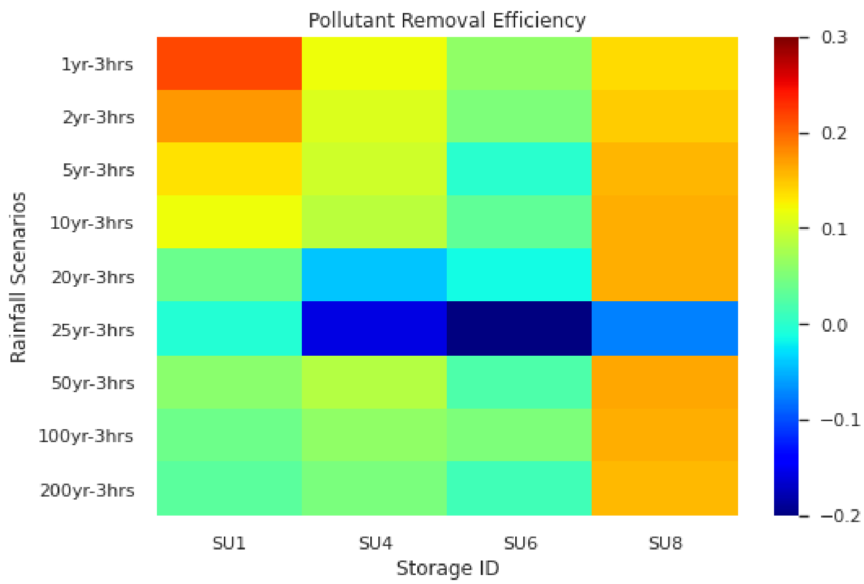


(c)

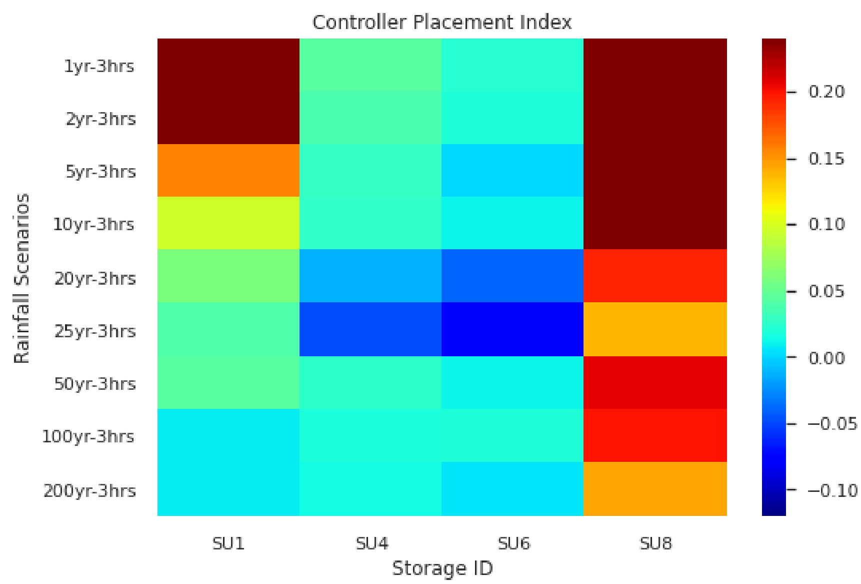


(d)

Fig.8. Heatmap of Controller Site Suitability Analysis by Considering: (a) Peak Depth Shaving Efficiency, (b) Flooded-hour Reduction, (c) Pollutant Removal Efficiency, (d) Controller Placement Index CPI under Various Designed Rainfall Events.

Overall, the selected controller 1 has the highest CPI, followed by controller 8 and controller 6, while controller 4 has the lowest CPI value. Only two storage units including SU4 and SU6, are suggested to keep open, which is in agreement with Wong and Kerkez (2018).Our results provide compelling evidence for controller site selection. However, some drawbacks are worth noting. Although the research goals were achieved to some extent, maximizing the global benefits by removing controller 6 and controller 4 is not validated. Still, Fig.7 shows that there are some abnormal behaviors resulting in negative PDSE, FRE, and FR. One of the reasons for this phenomenon was partially explained by Bartos and Kerkez (2019), who discovered how controller placements can shave peak hydraulic depth by using a graph-theoretic algorithm. In this urbanized catchment, increased flows were found to be closely tied to increased concentrations of total suspended solids. Future work, therefore, will step forward to investigate how flooding and pollutant loading diminishes after removing controller 6 and controller 4.

## 5. Limitations

This work was completed mainly based on co-simulating a ruled-based control strategy and urban drainage network A rainfall-runoff process by using the modified PySWMM. The first limitation of this study is the lack of fieldwork to verify modeled controllers' performance. Measurements and field testing in the future will play as a real-world testbed for the modeling outcomes in this paper. Secondly, controller settings of system-level control scenario 4 in Table 4 were determined by manual 'trial and error' procedure, which is labor-intensive work. Online optimized control algorithms such as model predictive control (Lund et al., 2018) and fuzzy logic control (Mounce et al., 2019; Zamani Sabzi et al., 2016) could be helpful for reducing the computational expense. Thirdly, it should be noticed that this water depth-based controller setting has limited contribution to remove TSS concentration (Fig.7c). Although real-time control strategy based on water depth of detention pond could improve pollutant removal efficiency 40-90% (Gaborit et al., 2016), it is arguable that the performance of hydraulic-dependent controller to realize the water quality objectives varies from case to case (Ascott et al., 2016; Grayson et al., 1997; Sharma et al., 2016). Finally, forecasting information on water quality was ignored in this work. Forecasts enable the RTC to flexibly and selectively discharge storm volume before extreme events; this allows the UDSs more capacity to withstand threats as well as failures. Future research recommends applying the forecasted data for improving RTC performance.

## 6. Conclusions

This study developed water quality simulation functionalities for PySWMM, which can be utilized to co-simulate control rules and water quality step-by-step. This co-simulation procedure was conducted under four control scenarios (no control, downstream individual control, system-level control with 11 same controllers, system-level control with 11 different controllers). Furthermore, the performance of each control strategy was assessed on the basis of three indicators including peak depth shaving efficiency (PDSE), pollutant removal efficiency (PRE), and flooded-hour reduction (FR). Finally, the controller sites of system-level control scenarios were selected by analyzing the Controller Placement Index (CPI). This co-simulation study provides insight into how system-level RTC can improve global water quantity and quality benefits. In summary, three pieces of conclusions were drawn below:

1) The new functionality enables to co-simulate water quality and control logics as a step-wise approach by using PySWMM. This co-simulation achievement allows researchers and engineers to consider water quality improvement as the metrics for controller performance and controller site selection.

2) Controller performance assessment shows that system-level control with 11 different controllers obtains the PDSE value up to 7.30%, PRE up to 66.59%, and FR up to 71.01%. system-level control with 11 different controllers outperforms other control strategies in global benefits such as flooding mitigation and TSS removal. However, compared with system-level control with 11 same controllers, system-level control with 11 different controllers is more likely to cause system instability because of more operation energy consumption. In contrast, the downstream individual control strategy is more capable of reducing flooding duration in the downstream sites.
3) Considering the pollutant removal as one of the components, CPI gets the trade-off between water quantity and quality. In order to maximize the global benefits, the results of the CPI heat map emphasized that only orifice 1 and 8 need to keep real-time regulated. This CPI-based controller placement analysis extended the method of Wong and Kerkez (2018), which is more reliable to select a suitable site for controllers placement.

## Declaration of interests

The authors declare that they have no known competing financial interests or personal relationships that could have appeared to influence the work reported in this paper

## Acknowledgments

This research was financially supported from the Smart Canal project of the USPCAS-W: US-Pakistan Center for Advanced Studies in Water. We want to show our thanks for Bryant

McDonnell, who are the major developers of PySWMM, for their assistance in PySWMM coding work. We would like to thank Branko Kerkez and Abhiram Mullapudi from the real-time water system group of the University of Michigan, for sharing the relevant model and files. We also thank Martin Cuma, who is the research scientist of the center of high-performance computing at the University of Utah, for his continuous efforts and help in educating and guiding me to compile PySWMM to Linux Programming Environment for parallel computing.

# References

Abou Rjeily, Y., Abbas, O., Sadek, M., Shahrour, I., Hage Chehade, F., 2018. Model Predictive Control for optimising the operation of Urban Drainage Systems. J. Hydrol. 566, 558–565. https://doi.org/10.1016/j.jhydrol.2018.09.044

Alley, W.M., 1981. Estimation of impervious - area Washoff Parameters. Water Resour. Res. 17, 1161–1166. https://doi.org/10.1029/WR017i004p01161

Ascott, M.J., Lapworth, D.J., Gooddy, D.C., Sage, R.C., Karapanos, I., 2016. Impacts of extreme flooding on riverbank filtration water quality. Sci. Total Environ. https://doi.org/10.1016/j.scitotenv.2016.02.169

Bartos, M., Kerkez, B., 2019a. Hydrograph peak-shaving using a graph-theoretic algorithm for placement of hydraulic control structures. Adv. Water Resour. 127, 167–179. https://doi.org/10.1016/j.advwatres.2019.03.016

Bartos, M., Kerkez, B., 2019b. Hydrograph peak-shaving using a graph-theoretic algorithm for placement of hydraulic control structures. Adv. Water Resour. https://doi.org/10.1016/j.advwatres.2019.03.016

Bartos, M., Wong, B., Kerkez, B., 2018. Open storm: A complete framework for sensing and control of urban watersheds. Environ. Sci. Water Res. Technol. 4, 346–358. https://doi.org/10.1039/c7ew00374a

Berggren, K., Olofsson, M., Viklander, M., Svensson, G., Gustafsson, A.-M., 2012. Hydraulic Impacts on Urban Drainage Systems due to Changes in Rainfall Caused by Climatic Change. J. Hydrol. Eng. 17, 92–98.

https://doi.org/10.1061/(ASCE)HE.1943-5584.0000406

Bilodeau, K., Pelletier, G., Duchesne, S., 2018. Real-time control of stormwater detention basins as an adaptation measure in mid-size cities. Urban Water J. 15, 858–867. https://doi.org/10.1080/1573062X.2019.1574844

Campisano, A., Cabot Ple, J., Muschalla, D., Pleau, M., Vanrolleghem, P.A., 2013. Potential and limitations of modern equipment for real time control of urban wastewater systems. Urban Water J. https://doi.org/10.1080/1573062X.2013.763996

Carpenter, J.F., Vallet, B., Pelletier, G., Lessard, P., Vanrolleghem, P.A., 2014. Pollutant removal efficiency of a retrofitted stormwater detention pond. Water Qual. Res. J. Canada. https://doi.org/10.2166/wqrjc.2013.020

Casal-Campos, A., Fu, G., Butler, D., Moore, A., 2015. An Integrated Environmental Assessment of Green and Gray Infrastructure Strategies for Robust Decision Making. Environ. Sci. Technol. 49, 8307–8314. https://doi.org/10.1021/es506144f

Chiang, P.K., Willems, P., 2015. Combine Evolutionary Optimization with Model Predictive Control in Real-time Flood Control of a River System. Water Resour. Manag. 29, 2527–2542. https://doi.org/10.1007/s11269-015-0955-5

Creaco, E., Campisano, A., Fontana, N., Marini, G., Page, P.R., Walski, T., 2019. Real time control of water distribution networks: A state-of-the-art review. Water Res. https://doi.org/10.1016/j.watres.2019.06.025

Emerson, C.H., Welty, C., Traver, R.G., 2005. Watershed-scale evaluation of a system of storm water detention basins. J. Hydrol. Eng. https://doi.org/10.1061/(ASCE)1084-0699(2005)10:3(237)

Gaborit, E., Anctil, F., Pelletier, G., Vanrolleghem, P.A., 2016. Exploring forecast-based management strategies for stormwater detention ponds. Urban Water J. 13, 841–851. https://doi.org/10.1080/1573062X.2015.1057172

Gaborit, E., Muschalla, D., Vallet, B., Vanrolleghem, P.A., Anctil, F., 2013. Improving the performance of stormwater detention basins by real-time control using rainfall forecasts. Urban Water J. https://doi.org/10.1080/1573062X.2012.726229

Giordano, A., Spezzano, G., Vinci, A., Garofalo, G., Piro, P., 2014. A Cyber-Physical System for Distributed Real-Time Control of Urban Drainage Networks in Smart Cities. pp. 87–98. https://doi.org/10.1007/978-3-319-

11692-1_8

Grayson, R.B., Gippel, C.J., Finlayson, B.L., Hart, B.T., 1997. Catchment-wide impacts on water quality: The use of "snapshot" sampling during stable flow. J. Hydrol. https://doi.org/10.1016/S0022-1694(96)03275-1

Hashemy Shahdany, S.M., Taghvaeian, S., Maestre, J.M., Firoozfar, A.R., 2019. Developing a centralized automatic control system to increase flexibility of water delivery within predictable and unpredictable irrigation water demands. Comput. Electron. Agric. https://doi.org/10.1016/j.compag.2019.104862

Heusch, S., Ostrowski, M., 2015. Model Predictive Control with SWMM. J. Water Manag. Model. https://doi.org/10.14796/jwmm.r241-14

HRWC, 2013. Malletts creekshed report. URL https://www.hrwc.org/wpcontent/uploads/Malletts_8x11.5.pdf (accessed 5.15.19).

Kerkez, B., Gruden, C., Lewis, M., Montestruque, L., Quigley, M., Wong, B., Bedig, A., Kertesz, R., Braun, T., Cadwalader, O., Poresky, A., Pak, C., 2016. Smarter stormwater systems. Environ. Sci. Technol. https://doi.org/10.1021/acs.est.5b05870

Kroll, S., Fenu, A., Wambecq, T., Weemaes, M., Van Impe, J., Willems, P., 2018. Energy optimization of the urban drainage system by integrated real-time control during wet and dry weather conditions. Urban Water J. 15, 362–370. https://doi.org/10.1080/1573062X.2018.1480726

Li, J., Burian, S., Oroza, C., 2019a. Exploring the potential for simulating system-level controlled smart stormwater system, in: World Environmental and Water Resources Congress 2019: Water, Wastewater, and Stormwater; Urban Water Resources; and Municipal Water Infrastructure - Selected Papers from the World Environmental and Water Resources Congress 2019.

Li, J., Tao, T., Kreidler, M., Burian, S., Yan, H., 2019b. Construction Cost-Based Effectiveness Analysis of Green and Grey Infrastructure in Controlling Flood Inundation: A Case Study. J. Water Manag. Model. https://doi.org/10.14796/jwmm.c466

Löwe, R., Vezzaro, L., Mikkelsen, P.S., Grum, M., Madsen, H., 2016. Probabilistic runoff volume forecasting in risk-based optimization for RTC of urban drainage systems. Environ. Model. Softw. 80, 143–158.

https://doi.org/10.1016/j.envsoft.2016.02.027

Lund, N.S.V., Borup, M., Madsen, H., Mark, O., Arnbjerg-Nielsen, K., Mikkelsen, P.S., 2019. Integrated stormwater inflow control for sewers and green structures in urban landscapes. Nat. Sustain. https://doi.org/10.1038/s41893-019-0392-1

Lund, N.S.V., Falk, A.K.V., Borup, M., Madsen, H., Steen Mikkelsen, P., 2018. Model predictive control of urban drainage systems: A review and perspective towards smart real-time water management. Crit. Rev. Environ. Sci. Technol. https://doi.org/10.1080/10643389.2018.1455484

McDonnell, B., M. Tryby, L. Montestruque, R. Kertesz, F.M., 2017. SWMM5 Application Programming Interface and PySWMM: A Python Interfacing Wrapper. Toronto, Canada.

Meneses, E.J., Gaussens, M., Jakobsen, C., Mikkelsen, P.S., Grum, M., Vezzaro, L., 2018. Coordinating rule-based and system-wide model predictive control strategies to reduce storage expansion of combined urban drainage systems: The case study of Lundtofte, Denmark. Water (Switzerland). https://doi.org/10.3390/w10010076

Mollerup, A.L., Mikkelsen, P.S., Thornberg, D., Sin, G., 2017. Controlling sewer systems–a critical review based on systems in three EU cities. Urban Water J. 14, 435–442. https://doi.org/10.1080/1573062X.2016.1148183

Mounce, S.R., Shepherd, W., Ostojin, S., Abdel-Aal, M., Schellart, A.N.A., Shucksmith, J.D., Tait, S.J., 2019. Optimisation of a fuzzy logic-based local real-time control system for mitigation of sewer flooding using genetic algorithms. J. Hydroinformatics. https://doi.org/10.2166/hydro.2019.058

Mullapudi, A., Bartos, M., Wong, B., Kerkez, B., 2018. Shaping streamflow using a real-time stormwater control network. Sensors (Switzerland) 18. https://doi.org/10.3390/s18072259

Mullapudi, A., Wong, B.P., Kerkez, B., 2017. Emerging investigators series: Building a theory for smart stormwater systems. Environ. Sci. Water Res. Technol. https://doi.org/10.1039/c6ew00211k

Muschalla, D., Vallet, B., Anctil, F., Lessard, P., Pelletier, G., Vanrolleghem, P.A., 2014. Ecohydraulic-driven real-time control of stormwater basins. J. Hydrol. https://doi.org/10.1016/j.jhydrol.2014.01.002

NRCS, 1986. Urban Hydrology for Small Watersheds TR-55. USDA Nat. Resour. Conserv. Serv. Conserv. Engeneering Div. Tech. Release 55. https://doi.org/Technical Release 55

Parolari, A.J., Pelrine, S., Bartlett, M.S., 2018. Stochastic water balance dynamics of passive and controlled stormwater basins. Adv. Water Resour. 122, 328–339. https://doi.org/10.1016/j.advwatres.2018.10.016

Riaño-Briceño, G., Barreiro-Gomez, J., Ramirez-Jaime, A., Quijano, N., Ocampo-Martinez, C., 2016. MatSWMM - An open-source toolbox for designing real-time control of urban drainage systems. Environ. Model. Softw. 83, 143–154. https://doi.org/10.1016/j.envsoft.2016.05.009

Rossman, L.A., 2015. STORM WATER MANAGEMENT MODEL USER'S MANUAL Version 5.1. EPA/600/R-14/413b, Natl. Risk Manag. Lab. Off. Res. Dev. United States Environ. Prot. Agency, Cincinnati, Ohio.

Ruggaber, T.P., Talley, J.W., Montestruque, L.A., 2007. Using embedded sensor networks to monitor, control, and reduce CSO events: A pilot study. Environ. Eng. Sci. https://doi.org/10.1089/ees.2006.0041

Sadler, J.M., Goodall, J.L., Behl, M., Morsy, M.M., 2019a. Leveraging Open Source Software and Parallel Computing for Model Predictive Control Simulation of Urban Drainage Systems Using EPA-SWMM5 and Python, in: Green Energy and Technology. https://doi.org/10.1007/978-3-319-99867-1_170

Sadler, J.M., Goodall, J.L., Behl, M., Morsy, M.M., Culver, T., Bowes, B.D., 2019b. Leveraging open source software and parallel computing for model predictive control of urban drainage systems using EPA-SWMM5. Environ. Model. Softw. https://doi.org/10.1016/j.envsoft.2019.07.009

Santon, R., 2018. $160M worth of projects could address Ann Arbor stormwater issues. URL https://www.mlive.com/news/ann-arbor/2018/01/160m_worth_of_projects_could_a.html (accessed 11.15.19).

Schmitt, T.G., Thomas, M., Ettrich, N., 2004. Analysis and modeling of flooding in urban drainage systems. J. Hydrol. 299, 300–311. https://doi.org/10.1016/S0022-1694(04)00374-9

Sharior, S., McDonald, W., Parolari, A.J., 2019. Improved reliability of stormwater detention basin performance through water quality data-informed real-time control. J. Hydrol. 573, 422–431. https://doi.org/10.1016/j.jhydrol.2019.03.012

Sharma, A.K., Vezzaro, L., Birch, H., Arnbjerg-Nielsen, K., Mikkelsen, P.S., 2016. Effect of climate change on stormwater runoff characteristics and treatment efficiencies of stormwater retention ponds: a case study from Denmark using TSS and Cu as indicator pollutants. Springerplus. https://doi.org/10.1186/s40064-016-3103-7

Shishegar, S., Duchesne, S., Pelletier, G., 2019. An Integrated Optimization and Rule-based Approach for Predictive Real Time Control of Urban Stormwater Management Systems. J. Hydrol. https://doi.org/10.1016/j.jhydrol.2019.124000

SMITH, C., 2015. City of ann arbor stormwater model calibration and analysis project-final report. URL https://www.a2gov.org/departments/systems-planning/planning-areas/waterresources/Documents/A2_SWM_Report_20150601 (accessed 4.27.19).

Sullivan, R.H., Manning, M.J., Heaney, J.P., Huber, W.C., Medina, Maj., 1977. Nationwide Evaluation of Combined Sewer Overflows and Urban Stormwater Discharges. Volume I: Executive Summary. Available from Natl. Tech. Inf. Serv. Springf. VA 22161 as PB-273 133, Price codes A10 Pap. copy, A01 Microfich. Rep. EPA-600/2-77-064a, Sept. 1977, 95 p. 13 fig, 31 tab. 68-03-0283.

U.S. EPA, 2006. Real time control of urban drainage networks.

van Overloop, P.J., Schuurmans, J., Brouwer, R., Burt, C.M., 2005. Multiple-model optimization of proportional integral controllers on canals. J. Irrig. Drain. Eng. https://doi.org/10.1061/(ASCE)0733-9437(2005)131:2(190)

Vezzaro, L., Grum, M., 2014. A generalised Dynamic Overflow Risk Assessment (DORA) for Real Time Control of urban drainage systems. J. Hydrol. https://doi.org/10.1016/j.jhydrol.2014.05.019

Vitasovic, Z.C., 2006. Real Time Control of Urban Drainage Networks 96.

Waters, D., Watt, W.E., Marsalek, J., Anderson, B.C., 2003. Adaptation of a storm drainage system to accomodate increased rainfall resulting from climate change. J. Environ. Plan. Manag. 46, 755–770. https://doi.org/10.1080/0964056032000138472

Wong, B.., 2017. Real-time Measurement and Control of Urban Stormwater Systems. University of Michigan, Ann Arbor.

Wong, B.P., Kerkez, B., 2018. Real-Time Control of Urban Headwater Catchments Through Linear Feedback: Performance, Analysis, and Site Selection. Water Resour. Res. 54, 7309–7330. https://doi.org/10.1029/2018WR022657

Zamani Sabzi, H., Humberson, D., Abudu, S., King, J.P., 2016. Optimization of adaptive fuzzy logic controller using novel combined evolutionary algorithms, and its application in Diez Lagos flood controlling system, Southern New Mexico. Expert Syst. Appl. 43, 154–164. https://doi.org/10.1016/j.eswa.2015.08.043

Zhang, P., Cai, Y., Wang, J., 2018. A simulation-based real-time control system for reducing urban runoff pollution through a stormwater storage tank. J. Clean. Prod. https://doi.org/10.1016/j.jclepro.2018.02.130